Catalysis Today 164 (2011) 528–532

Contents lists available at ScienceDirect

Catalysis Today

journal homepage: www.elsevier.com/locate/cattod

Catalytic decomposition of ammonia in simulated coal-derived gas over supported nickel catalysts

Yasushi Ozawa*, Yoshihisa Tochihara

Energy Engineering Research Laboratory, Central Research Institute of Electric Power Industry, 2-6-1 Nagasaka, Yokosuka, Kanagawa 240-0196, Japan

ARTICLE INFO

Article history:
Received 30 June 2010
Received in revised form
16 November 2010
Accepted 17 November 2010
Available online 15 December 2010

Keywords:
IGCC
Hot gas clean-up
Ammonia decomposition
Catalysis
Catalyst selectivity

ABSTRACT

As a hot gas clean-up technology for integrated coal gasification combined-cycle (IGCC) power plants, the catalytic decomposition of ammonia using simulated coal-derived gas was studied. Based on the selective catalytic oxidation of ammonia to nitrogen and water, the characteristics of five kinds of supported nickel catalysts were investigated. Ammonia decomposition experiments were carried out at 0.9 MPa, and the surface properties of the catalysts were investigated through surface area measurement, the temperature programmed desorption of ammonia (NH_3-TPD), carbon analysis, XRD analysis, and transmission electron microscope (TEM) observation. The results showed that a nickel catalyst supported on ZSM-5 zeolite has the highest activity and selectivity for ammonia decomposition to nitrogen without carbon deposition from 250–400 °C among the tested catalysts.

1. Introduction

Coal fuel is important energy source for power generation because of its abundance and inexpensive price, while its disadvantage is its high level of carbon dioxide (CO_2) emissions. However, when compared to conventional systems, IGCC is a high-efficiency power generation system using coal fuel with lower CO_2 emissions. Against this backdrop, the Japanese government and electric power companies are currently conducting a pilot project using a 250 MW IGCC, which mainly consists of an oxygen-enriched air blown-type gasifier, a wet cleanup, a gas turbine, and a steam turbine [1]. The fuel from the air-blown gasification of coal contains ammonia (NH_3), which causes the emission of harmful NO_x from the gas turbine. The wet cleanup has the potential to reduce NH_3 as well as sulfur compounds, but reduces thermal efficiency. In contrast, a dry cleanup is an advanced technology that does not reduce thermal efficiency [2]. Among the dry processes of NH_3 removal, catalytic decomposition is a promising technology [3]. The catalytic reactor for decomposing NH_3 could benefit from the high reaction temperature at the exit of the gasifier, while the catalyst must be tolerant to particulates, H_2S, and other contaminants [3]. Mojtahedi et al. reported that the catalytic activities of all the tested catalysts decreased after 20 h of coal gasification tests, probably due to the decline in the specific surface area of the catalysts and the presence of H_2S in the gasifier gas [4]. On the contrary, the location at the exit of the desulfurizer and particulate filter has the advantage of prolonging catalyst life, but has the disadvantage of lowering the NH_3 decomposition rate because of low temperature.

In recent years, the selective catalytic oxidation of NH_3 at low temperature has been widely investigated due to increasing environmental concerns [5–8]. Although most of these studies have been carried out under restricted conditions, the performance of NH_3 decomposition is influenced by the reaction conditions, e.g., fuel composition [9]. Under these circumstances, we studied the selective catalytic oxidation of NH_3 in simulated coal-derived gas and revealed the potential of supported nickel (Ni) catalysts [10]. Additionally, the acidity of the catalyst also plays a critical role in the selective catalytic oxidation of NH_3 [11], and the same applies to coke deposition leading to catalyst deactivation [12]. Furthermore, Ni catalyzes carbon formation reactions [13], and we reveal that the addition of small amounts of oxygen to the fuel significantly reduces carbon formation on supported Ni catalysts [10]. In this study, we report the effect of the materials supported by Ni for the selective catalytic decomposition of NH_3 in simulated coal-derived gas under a pressurized condition.

2. Experimental

Ni catalysts supported on alumina (Ni/Al), silica–alumina (Ni/SiAl), Y zeolite (Ni/zY), β zeolite (Ni/zB), and ZSM-5 zeolite (Ni/z5) were prepared using an impregnation method (Table 1). In the previous report by Mihindow-Koumba et al. [14], the cok-

* Corresponding author. Tel.: +81 46 856 2121; fax: +81 46 856 3346.
E-mail address: ozaway@criepi.denken.or.jp (Y. Ozawa).

0920-5861/$ – see front matter © 2010 Elsevier B.V. All rights reserved.
doi:10.1016/j.cattod.2010.11.037

Table 1
Characterization of the catalysts.

Sample	Ni content [μmol/g-support]	Support	BET surface area [m^2/g]	Pore volume [ml/g]	Mean pore diameter [nm]
Ni/Al	250	Al_2O_3	148	0.64	17
Ni/SiAl	250	71.06% SiO_2 + 28.61% Al_2O_3	418	0.83	8
Ni/zY	250	Y zeolite (SiO_2/Al_2O_3 = 5.7 mol/mol)	726	0.41	2
Ni/zB	250	β zeolite (SiO_2/Al_2O_3 = 390 mol/mol)	570	0.37	3
Ni/z5	250	ZSM-5 zeolite (SiO_2/Al_2O_3 = 39 mol/mol)	388	0.19	2

ing amount on HBEA (β zeolite), HMFI (ZSM-5 zeolite), and HFAU (Y zeolite) with an Si/Al ratio of 15 was added the following order: HBEA > HMFI > HFAU. In general, coke deposition on zeolite decreases with decreasing acidity [12], which is attributed to the Al ratio in a zeolite framework. Accordingly, high Si/Al ratios of β zeolite and low Si/Al ratios of Y zeolite, compared to ZSM-5 zeolite, were selected. Alumina powder (AKP-G015, Sumitomo Chemical), powdered silica–alumina pellet (JRC-SAH-1, Catalysis Society of Japan), Y zeolite power (HSZ-320HOA, Tosoh), β zeolite power (HSZ-980HOA, Tosoh), and ZSM-5 zeolite powder (HSZ-840NHA, Tosoh) were respectively impregnated with an aqueous solution of $Ni(NO_3)_2{\cdot}6H_2O$ (Wako Junyaku), and were then stirred and dried. The samples were then heated to 500 °C at the rate of 300 °C h^{-1} within an air flow through a silica gel trap, calcined at 500 °C for 5 h, and then cooled to room temperature. The resulting solid was molded, crushed, and sieved through a JIS 2–3 mm mesh.

The BET surface area and mean pore diameter of the catalysts were measured using N_2 physisorption (BELL SORP max, Bell Japan) after being dried in a vacuum condition for 3 h at 300 °C. NH_3-TPD was then carried out utilizing a Bell Japan TPD-1-AT in an He stream at 10 °C min^{-1} from 100 °C to 600 °C while being analyzed with a quadrupole mass spectrometer from m/z = 16, after pretreatment at 500 °C for 1 h using an He stream and after NH_3 adsorption at 100 °C. The dispersion of Ni was measured by the CO pulse method at 50 °C using an Ohkura Riken R6015 after being reduced in an H_2 stream for 2 h at 700 °C or 800 °C. The Ni particle diameter was calculated using a CO:Ni stoichiometry factor of 1.

NH_3 decomposition was carried out using a conventional fixed-bed flow reactor made of Inconel® alloy with an inner quartz glass tube with 3.6 ml of the catalyst at 0.9 MPa. Following N_2 introduction for 2 h up to 150 °C, simulated coal-derived gas fuel (H_2 = 10.5 mol%, CO = 28.4 mol%, N_2 = 54.3 mol%, CO_2 = 3.6 mol%, H_2O = 3.1 mol%, and NH_3 = 0.104 mol%) was introduced into the reactor at the space velocity of 20,000 h^{-1}. Then, 0.008 mol/mol-fuel of O_2 was added to the fuel, and the catalyst was stepwise heated from 150 °C to 600 °C. The total reaction time was 6 h. For the reaction products, NH_3, HCN, NO, NO_2, and N_2O were measured using an FT-IR (FT-730G, Horiba), in which a gas flow passage was heated, and H_2, N_2, O_2, CO, CO_2, CH_4, C_2H_4, C_2H_6, C_3H_6, C_3H_8, i-C_4H_{10}, and n-C_4H_{10} were measured using a micro-TCD (CP4900, Varian) connected online. The N_2O concentration was corrected with a CO_2 concentration to cancel the CO_2 interference. Then, the NH_3 conversion to N_2 was calculated using $(C[NH_3in]–C[\Sigma XN])/C[NH_3in] \times 100\%$, where $C[NH_3in]$ was the inlet molar concentration of NH_3 and where $C[\Sigma XN]$ was the outlet molar concentration of the total nitrogenous compounds (NH_3 + NO + NO_2 + N_2O + HCN). Similarly, the conversion to NO, NO_2, N_2O, or HCN was calculated using $C[N_x]/C[NH_3in] \times 100\%$, where $C[N_x]$ was the outlet molar concentration of NO, NO_2, N_2O, or HCN. The amount of carbon deposited on the catalysts during NH_3 decomposition was measured using a CHN analyzer (2400 Series II, PerkinElmer). The XRD spectra of the powdered catalysts before and after NH_3 decomposition were taken using a Rigaku RINT TTRIII with a Cu Kα radiation source (λ = 1.540562 Å) and identified using a PDF database. The average crystallite size (D) of the metallic Ni was calculated using the Scherrer method, $D = 0.9\lambda/\beta\cos\theta$, where β was the full width at half maximum of the Ni (1 1 1) peak at 2θ = 44.51°. The TEM images were taken using a JEOL JEM-2100F operated at 200 kV. At the same time, Ni, C, Al, and O were detected using energy-dispersive X-ray spectroscopy (EDX). For the TEM observation, samples were ground and dispersed in ethanol by supersonic waves and put on Cu grids with polymer-supporting film.

3. Results and discussion

3.1. Surface properties

The BET surface area, pore volume, and mean pore diameter of the catalysts are shown in Table 1. Ni/Al showed the smallest surface area, a large pore volume, and the largest mean pore diameter. Meanwhile, Ni/SiAl showed medium surface area, medium mean pore diameter, and the largest pore volume, and Ni/zY and Ni/zB showed a large surface area, medium pore volume, and small mean pore diameter. Lastly, Ni/z5 showed the smallest mean pore diameter, but had the smallest pore volume and a medium surface area. The NH_3-TPD results of the catalysts are summarized in Table 2. Two apparent NH_3 desorption peaks were observed for Ni/z5, while the peak was not apparently divided for the other catalysts. Both the total acid amount and strong acid amount [15], calculated by the NH_3 desorption amount at or above 250 °C, decreased in the order of Ni/z5 >> Ni/zY > Ni/SiAl > Ni/Al > Ni/zB. Meanwhile, the order of the temperature of the maximum NH_3 desorption (in the higher temperature peak between the two desorption peaks for Ni/z5) was Ni/z5 >> Ni/zB > Ni/Al > Ni/SiAl > Ni/zY. These results indicate that Ni/z5 has the strongest acidity among the prepared catalysts. As the dispersion of Ni has the possibility of affecting selective catalytic oxidation of NH_3 and carbon deposition, we tried to analyze Ni dispersion. However, we were not able to detect it after H_2 reduction for 2 h at 700 °C for all the catalysts, with the same result at 2 h at 800 °C, excluding Ni/Al. The Ni particle diameter for Ni/Al was 17 nm, assuming that CO was adsorbed on all the Ni. This value may be inaccurate because NiO reduction for such a low nickel loading catalyst as Ni/Al could be incomplete at this temperature [16], while a higher temperature would be unfavorable, due to metal sintering and the change of the support structure. Compared to Ni/Al, the other catalysts would have stronger interaction with NiO on the support structure because of the lack of reduction under 800 °C.

Table 2
NH_3-TPD results of the catalysts.

Sample	Total acid amount [mmol/g]	Acid amount (≥250 °C) [mmol/g]	NH_3 desorption peak temperature [°C]
Ni/Al	0.23	0.12	257
Ni/SiAl	0.36	0.17	205
Ni/zY	0.69	0.26	193
Ni/zB	0.11	0.08	274
Ni/z5	1.30	0.82	371[a]

[a] Peak of higher temperature between two peaks.

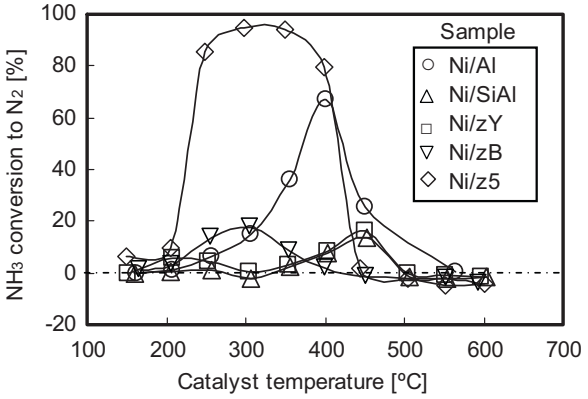

Fig. 1. NH_3 conversion to N_2 during NH_3 decomposition; H_2 = 10.5 mol%, CO = 28.4 mol%, N_2 = 54.3 mol%, CO_2 = 3.6 mol%, H_2O = 3.1 mol%, NH_3 = 0.104 mol%, O_2/fuel = 0.008 mol/mol, S.V. = 20,000 h^{-1}, pressure = 0.9 MPa.

3.2. NH_3 decomposition performance and influence on fuel composition

Fig. 1 shows the NH_3 conversion to N_2 during NH_3 decomposition using simulated coal-derived gas under the conditions of an O_2/fuel mol/mol ratio of 0.008 and a pressure of 0.9 MPa. In the case of Ni/Al and Ni/zB, the catalyst bed temperature exceeded the set value at 500 °C because of the occurrence of a large exothermic reaction, thus the data was taken at the settled temperature. Ni/SiAl, Ni/zY, and Ni/zB showed low NH_3 conversion to N_2. Ni/Al showed a 67% conversion of NH_3 at 400 °C, while the temperature range of the high NH_3 conversion was narrow. In contrast, Ni/z5 showed the highest NH_3 conversion to N_2 above 79%, over a wider temperature range from 250 °C to 400 °C, and above 94% from 300 °C to 350 °C. These results correspond to the previous results that the order of the conversion and selectivity was Fe-ZSM-5 > Fe-Beta by Akah et al. [8] and Fe-ZSM-5 > Fe-Y > Fe-Beta by Long et al. [17], while these metallic elements did not consist of Ni. As shown in Table 2, Ni/z5 has the strongest acidity, while Ni/Al has a certain level of acidity. Akah et al. reported that catalysts with no Al and hence possessing only weak acidity had lower performance during the selective catalytic oxidation of NH_3 [11]. Thus, the strongest acidity would also affect the performance of selective NH_3 decomposition over Ni/z5.

Fig. 2 shows the NH_3 conversion to HCN during NH_3 decomposition. The conversion to HCN increased with increasing temperature, and the order of the conversion was Ni/z5 < Ni/zB, Ni/zY < Ni/Al < Ni/SiAl. Especially for Ni/z5, HCN was not observed

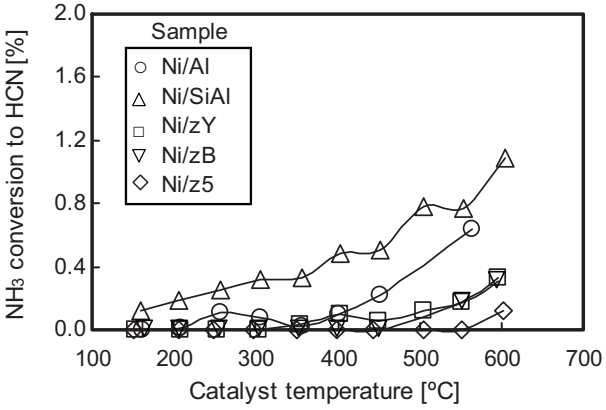

Fig. 2. NH_3 conversion to HCN during NH_3 decomposition; test conditions shown in Fig. 1.

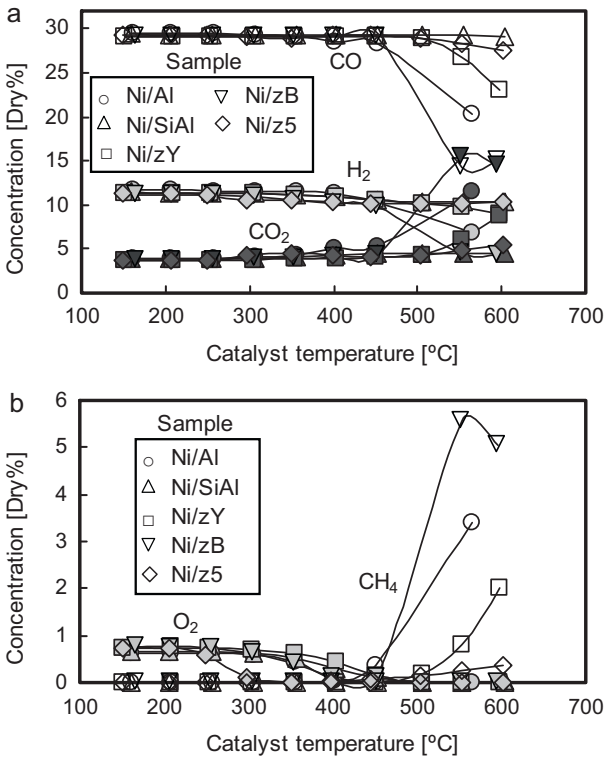

Fig. 3. Changes in (a) H_2, CO and CO_2 concentrations and (b) O_2 and CH_4 concentrations in the catalyst outlet gas during NH_3 decomposition; test conditions shown in Fig. 1.

up to 550 °C. For all the catalysts, NH_3 conversion to NO was below 0.10%, which is below the reliable detection limit of the analyzer, and only a small amount of NH_3 was converted to NO_2 up to 0.25%; with N_2O up to 0.22%. This high selectivity of NH_3 to N_2 agrees with the study by Leppälahti et al. [5] regarding NH_3 selective oxidation in synthetic gasification gas. In contrast, Long et al. reported the result of selective oxidation in NH_3, O_2, and He mixtures, in which Ni-ZSM-5 showed high selectivity to NO among the tested various metal-ZSM-5 catalysts [18]. Meanwhile, Olofsson et al. reported that selectivity of NH_3 to N_2 increased with the addition of CO, H_2, and H_2O to N_2 at 0.5% O_2 over $Pt/CuO/Al_2O_3$ [9]. Furthermore, Nassos et al. demonstrated that NO and NO_2 emissions were only a few ppm at low O_2 concentration and low space velocity in the selective catalytic oxidation of NH_3 in a gasified biomass, while increasing O_2 concentration and space velocity led to increasing NO and NO_2 [19]. This indicates that the NH_3 is first oxidized to NO, which is then reduced to N_2 [19], and NO reduction to N_2 is extremely fast in low O_2 concentration. Thus, the composition of coal-derived gas including CO, H_2, and H_2O with low O_2 concentration and low space velocity would be favorable for the selectivity to N_2 for the tested catalysts.

Fig. 3 shows the changes in H_2, CO, CO_2, O_2, and CH_4 concentrations in the catalyst outlet gas. For Ni/z5, Ni/zB, and Ni/Al, O_2 concentration decreased with increasing NH_3 conversion to N_2 (Fig. 1), indicating the progress of the selective catalytic oxidation of NH_3 ($4NH_3 + 3O_2 \rightarrow 2N_2 + 6H_2O$). However, H_2 concentration also decreased slightly with decreasing O_2 concentration for Ni/z5, and CO concentration did the same for Ni/Al, indicating the simultaneous oxidation of H_2 and CO, respectively. Subsequently, the H_2 and/or CO concentration for Ni/z5, Ni/zB, and Ni/Al decreased with decreasing NH_3 conversion to N_2, indicating that the oxidation of H_2 and/or CO gained ascendancy over NH_3 oxidation. Further, CO and CO_2 concentrations were approximately constant up to 600 °C for Ni/SiAl, whereas the concentrations for Ni/zB and

Table 3
Carbon deposition and crystallite size of metallic Ni in the catalysts after NH_3 decomposition from 150 °C to 600 °C at 0.9 MPa for 6 h.

Sample	Carbon deposition [wt%]	Crystallite size [nm]
Ni/Al	13.43	49
Ni/SiAl	0.02	29
Ni/zY	0.13	35
Ni/zB	26.83	31
Ni/z5	0.07	48

Ni/Al began to change at 400 °C, and then markedly changed above 500 °C. Concerning Ni/zY and Ni/z5, these concentrations began to change at 500 °C. The order of the changes of CO and CO_2 concentrations above 500 °C was Ni/SiAl < Ni/z5 < Ni/zY < Ni/Al < Ni/zB. Moreover, CH_4 formation was observed above 450 °C for Ni/Al and Ni/zB, and above 500 °C for Ni/zY and Ni/z5. The order of CH_4 concentration was the same as that of the changes of H_2, CO, and CO_2 concentrations, while CH_4 was not observed for Ni/SiAl, and the concentration for Ni/z5 stayed at a low level below 0.4% (dry). However, C_2H_4, C_2H_6, C_3H_6, C_3H_8, *i*-C_4H_{10}, and *n*-C_4H_{10} were scarcely observed for all the catalysts. These results indicate that both the carbon formation reaction (Boudouard reaction: $2CO \rightarrow C + CO_2$), which causes catalyst deactivation [12], and methanation reaction ($2CO + 2H_2 \rightarrow CH_4 + CO_2$), which causes fuel degradation, proceeded at higher temperatures, excluding Ni/SiAl. Additionally, it is revealed that the suitable temperature zone for the avoidance of carbon formation and methane formation was below 350 °C for Ni/Al and Ni/zB, and below 450 °C for Ni/zY and Ni/z5, whereas there was no limit for Ni/SiAl. This temperature zone includes the temperature of the maximum conversion of NH_3 to N_2 (Fig. 1) for Ni/SiAl, Ni/zB, and Ni/z5, and at the edge for Ni/zY, excluding Ni/Al. Thus, Ni/z5 has the highest activity for NH_3 decomposition to N_2 without carbon formation at 250–400 °C, while Ni/zB and Ni/SiAl show some capacity for NH_3 decomposition without carbon formation at around 300 °C and 450 °C, respectively. Meanwhile, carbon deposition is associated with the temperature of the maximum decomposition of NH_3 for Ni/Al at 400 °C.

Table 3 shows the carbon deposition on the catalysts after NH_3 decomposition from 150 °C to 600 °C for 6 h. The deposition increased in the order of Ni/SiAl < Ni/z5 < Ni/zY < Ni/Al < Ni/zB, which corresponds to the order of the changes of CO and CO_2 concentrations above 500 °C during NH_3 decomposition (Fig. 3(a)). These results support the fact that the carbon deposition occurred because of a Boudouard reaction. As compared with the surface properties of the catalysts (Tables 1 and 2), a strong correlation between the carbon deposition and the surface properties covered for all the catalysts was not indicated. However, it was revealed that the carbon deposition increased with increased mean pore diameter and with decreased acid amount in regard to Ni/zY, Ni/zB, and Ni/z5, which have a sharp distribution of pore size. The effect of acidity on coke formation in zeolite catalysts was previously investigated in a pyrolysis of vacuum gas oil and polyethylene blends, such that the order of the amount of coke formation was HZSM-5 (Si/Al: 22) < HBeta (Si/Al: 25) < HUSY (Si/Al: 4.8), and both the weak and total acid amounts of HUSY were larger than those of ZSM-5 [20]. The author mentioned that the higher coke amount of HUSY was possibly due to the high acidity associated with weak acid sites. In contrast, Ni/z5 had the strongest acidity in our result, despite the lowest coke deposition. Guisnet et al. wrote that the roles of strength and density in active acid sites are generally limited in comparison to the roles played by the size and shape of cavities and the size of their apertures [12]. Thus, steric constraints exerted by the pore network of Ni/z5 on the formation of coke intermediates would be responsible for low coke deposition [21].

Fig. 4 shows the XRD patterns of Ni/Al and Ni/z5, which were superior for NH_3 conversion among the tested catalysts, before and after NH_3 decomposition. From the XRD analysis of the catalysts after the NH_3 decomposition experiment, a large peak at $2\theta = 26.6°$ was identified as carbon (PDF#26-1080) for Ni/Al but not for Ni/z5. Ni or Ni compounds were not identified for Ni/Al and Ni/z5 before NH_3 decomposition. This indicates that NiO was well-dispersed on the support structure. However, trace peaks at $2\theta = 44.5°$ and 51.8° were identified as Ni metal (PDF#04-0850) for Ni/Al and Ni/z5 after NH_3 decomposition, indicating some agglomeration of metallic Ni. Additionally, the intensity of peaks at $2\theta = 8.0°$, 8.8°, 8.9°, 23.1°, and 23.3°, etc., as ZSM-5 (PDF#44-0003) grew higher for Ni/z5 after NH_3 decomposition, which indicated an increase in the crystallinity of ZSM-5. Although some peaks of SiO_2 (PDF#44-0696) overlapped with the peaks of ZSM-5, the intensity of the sole peaks of SiO_2 at $2\theta = 26.7°$ and 30.0° did not grow higher. The Ni agglomeration and the increase of the ZSM-5 crystallinity during NH_3 decomposition occur above the preparation temperature of the catalysts at 500 °C. From the XRD analysis of the other catalysts (not shown here), Ni (metal or compound) and carbon were not detected before NH_3 decomposition, while the trace peaks of Ni metal detected for all the catalysts and carbon were seen for Ni/zB after NH_3 decomposition. The average crystallite size of metallic Ni calculated from the small peak at $2\theta = 44.51°$ in the XRD pattern after NH_3 decomposition is shown in Table 3, where the peak was separated from the peak shoulder of Al_2O_3 for Ni/Al (Fig. 4(a)). A large crystallite size of Ni was calculated for Ni/Al and Ni/z5, which showed both high performances for the selective catalytic oxidation of NH_3. It is extrapolated that the catalysis for NH_3 decomposition would cause metallic Ni agglomeration on the catalyst, while the agglomerating Ni is of a small quantity because the peaks of Ni in XRD were quite small. However, there is likely no relation between Ni crystallite size and carbon formation because the particle size was similarly small for both the Ni/SiAl with a small amount of carbon formation and the Ni/zB with a large amount of carbon formation. Additionally, the particle size was similarly large for the Ni/z5 with a small

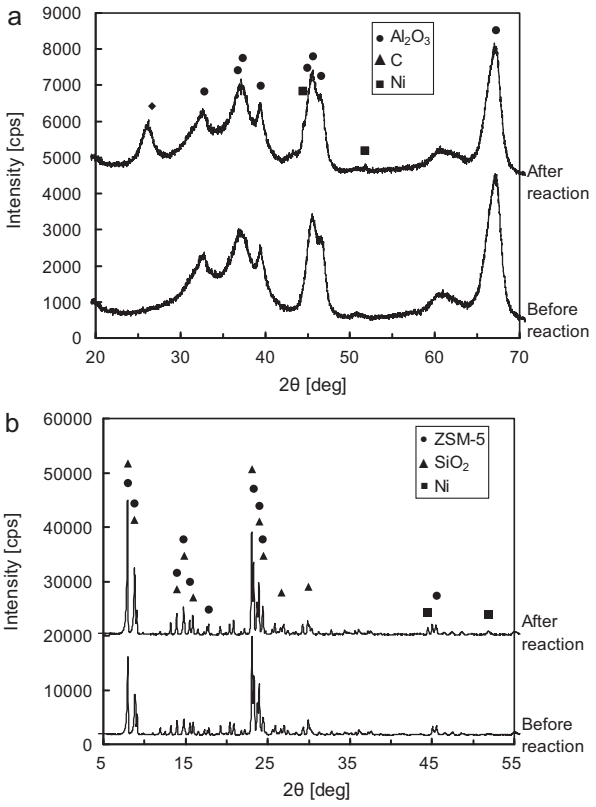

Fig. 4. XRD patterns of (a) Ni/Al and (b) Ni/z5 before and after NH_3 decomposition.

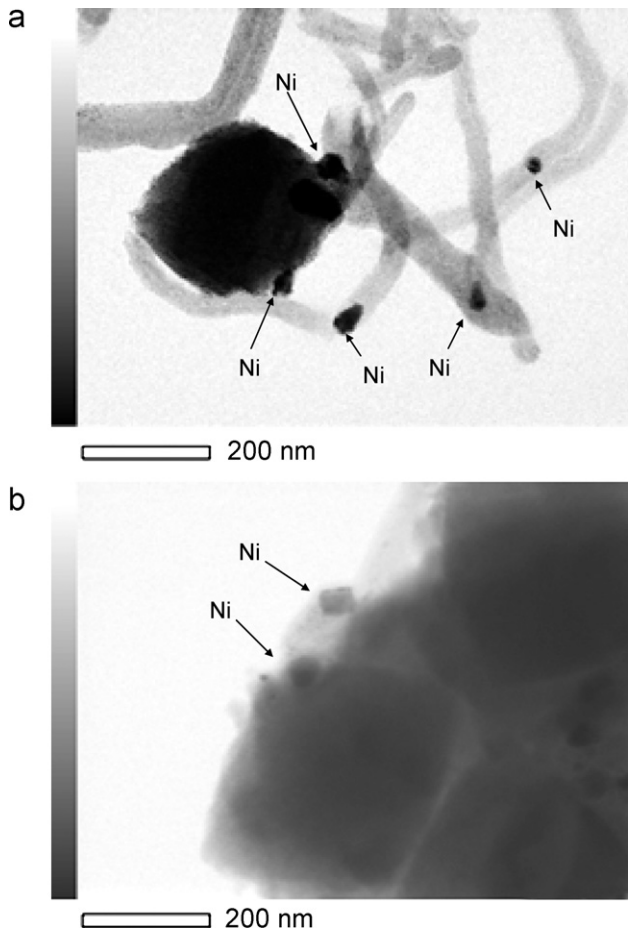

Fig. 5. TEM images of (a) Ni/zB and (b) Ni/z5 after NH_3 decomposition.

amount of carbon formation and the Ni/Al with a large amount of carbon formation. Fig. 5 shows the TEM images of Ni/zB and Ni/z5 after NH_3 decomposition. Considerable amounts of carbon filaments are observed for Ni/zB, and the filaments include Ni particles. In contrast, Ni particles are observed on the support structure without carbon filaments for Ni/z5. This fact suggests that on Ni/zB, Ni particles, agglomerated to a certain degree, move away from the catalyst surface with the growth of carbon filaments; then further agglomeration ceases, and small particles remain on the surface. These implications are not conflicting with Shaikhutdinov et al., which mentioned that optimum Ni size exists for filament growth [22]. Furthermore, the lack of carbon filaments on the Ni/z5 having large Ni particles indicates that the pore structure of the support structure would be more responsible for carbon filament formation than Ni particle size and support structure acidity.

4. Conclusions

The characteristics of the five kinds of supported Ni catalysts were studied to assess their potential for selective catalytic decomposition of NH_3 as a hot gas clean-up technology for IGCCs. A ZSM-5-supported Ni catalyst with fine pore diameter and the highest solid acidity has the highest activity and selectivity for NH_3 decomposition to N_2, and can inhibit carbon deposition and CH_4 formation at 250–400 °C among the tested catalysts. The strong acidity of the ZSM-5-supported Ni catalyst can affect the performance of NH_3 decomposition, and the composition of coal-derived gas including CO, H_2, and H_2O with low O_2 concentrations is favorable for the selectivity of NH_3 to N_2. Moreover, steric constraints exerted by the pore network of the ZSM-5-supported Ni catalyst on the formation of coke intermediates could be responsible for low coke deposition. An alumina-supported Ni catalyst with medium acidity has high activity while being associated with carbon deposition at the temperature of the maximum decomposition of NH_3 at 400 °C. A β zeolite-supported Ni catalyst with low acidity and a silica-alumina-supported Ni catalyst with medium acidity have some capacity to decompose NH_3 without carbon formation at around 300 °C and 450 °C, respectively.

References

[1] S. Kaneko, Y. Ishibashi, J. Wada, 250 MW air blown IGCC demonstration plant project, in: Proceeding of the International Conference on Power Engineering-03 (ICOPE-03), vol. 3, November 9–13, Kobe, 2003, pp. 163–167.
[2] T. Nakayama, S. Ito, H. Matsuda, H. Shirai, M. Kobayashi, T. Tanaka, H. Ishikawa, CRIEPI Rep. EW89015, 1990.
[3] G.N. Krishnan, B.J. Wood, A. Sanjurjo, DOE/MC/23087-2504, 1987.
[4] W. Mojtahedi, M. Ylitalo, T. Maunula, J. Abbasian, Fuel Process. Technol. 45 (1995) 221.
[5] J. Leppälahti, P. Kilpinen, M. Hupa, Energy Fuels 12 (1998) 758.
[6] L. Lietti, G. Ramis, G. Busca, F. Bregani, P. Forzatti, Catal. Today 61 (2000) 187.
[7] L. Gang, B.G. Anderson, J. van Grondelle, R.A. van Santen, Appl. Catal. B 40 (2003) 101.
[8] A.C. Akah, C. Cundy, A.A. Garforth, Appl. Catal. B 59 (2005) 221.
[9] G. Olofsson, L.R. Wallenberg, A. Andersson, J. Catal. 230 (2005) 1.
[10] Y. Ozawa, Y. Tochihara, Chem. Eng. Sci. 62 (2007) 5364.
[11] A.C. Akah, G. Nkeng, A.A. Garforth, Appl. Catal. B 74 (2007) 34.
[12] M. Guisnet, P. Magnoux, D. Martin, Stud. Surf. Sci. Catal. 111 (1997) 1.
[13] P.D.F. Vernon, M.L.H. Green, A.K. Cheetham, A.T. Ashcroft, Catal. Today 13 (1992) 417.
[14] P.C. Mihindou-Koumba, H.S. Cerqueira, P. Magnoux, M. Guisnet, Ind. Eng. Chem. Res. 40 (2001) 1042.
[15] K. Nishi, S. Komai, K. Inagaki, A. Satsuma, T. Hattori, Appl. Catal. A 223 (2002) 187.
[16] P. Kim, Y. Kim, H. Kim, I.K. Song, J. Yi, Appl. Catal A 272 (2004) 157.
[17] R.Q. Long, R.T. Yang, J. Catal. 201 (2001) 145.
[18] R.Q. Long, R.T. Yang, Chem. Commum. (2000) 1651.
[19] S. Nassos, E. Elm svensson, M. Boutonnet, S.G. Järås, Appl. Catal. B 74 (2007) 92.
[20] A. Marcilla, A. Gómez-Siurana, A.O. Odjo, R. Navarro, D. Berenguer, Polym. Degrad. Stab. 93 (2008) 723.
[21] M. Guisnet, P. Magnoux, Appl. Catal. 54 (1989) 1.
[22] S.K. Shaikhutdinov, L.B. Avdeeva, B.N. Novgorodov, V.I. Zaikovskii, D.I. Kochubey, Catal. Lett. 47 (1997) 35.